

**Reduction of intracerebral hemorrhage by rivaroxaban after tPA
thrombolysis is associated with down-regulation of PAR-1 and PAR-2**

Ryuta Morihara,¹ Toru Yamashita,¹ Syoichiro Kono,¹ Jingwei Shang,¹ Yumiko Nakano,¹
Kota Sato,¹ Nozomi Hishikawa,¹ Yasuyuki Ohta,¹ Stefan Heitmeier,² Elisabeth Perzborn,²
and Koji Abe¹

¹Departments of Neurology, Dentistry and Pharmaceutical Sciences, Graduate School of Medicine, Okayama University, Okayama, Japan

²Bayer Pharma AG, Drug Discovery - Global Therapeutic Research Groups, Cardiovascular Pharmacology, Wuppertal, Germany

Abbreviated title: Down-regulation of PAR-1 and PAR-2 by rivaroxaban

Name of Associate Editor: Jerome Badaut, PhD

KeyWords: PAR-3; PAR-4; tissue plasminogen activator; warfarin

Correspondence to

Koji Abe, MD, PhD,

Department of Neurology, Graduate School of Medicine, Dentistry and Pharmaceutical Sciences, Okayama University, 2-5-1 Shikata-cho Kita-ku, Okayama 700-8558, Japan.

Tel: +81-86-235-7365, **Fax:** +81-86-235-7368

E-mail: p2k07119@cc.okayama-u.ac.jp

Support or grant information: This work was mainly supported by Bayer Yakuhin, Ltd.

Abstract

This study aimed to assess the risk of intracerebral hemorrhage (ICH) after tissue-type plasminogen activator (tPA) treatment in rivaroxaban compared with warfarin pretreated male Wistar rat brain after ischemia in relation to activation profiles of protease-activated receptor-1, -2, -3, and -4 (PAR-1, -2, -3, and -4). After pretreatment with warfarin (0.2 mg/kg/day), low dose rivaroxaban (60 mg/kg/day), high dose rivaroxaban (120 mg/kg/day), or vehicle for 14 days, transient middle cerebral artery occlusion was induced for 90 min, followed by reperfusion with tPA (10 mg/kg/10 mL). Infarct volume, hemorrhagic volume, immunoglobulin G leakage, and blood parameters were examined. Twenty-four hours after reperfusion, immunohistochemistry for PARs was performed in brain sections. ICH volume was increased in the warfarin-pretreated group compared with the rivaroxaban-treated group. PAR-1, -2, -3, and -4 were widely expressed in the normal brain, and their levels were increased in the ischemic brain, especially in the peri-ischemic lesion. Warfarin pretreatment enhanced the expression of PAR-1 and PAR-2 in the peri-ischemic lesion, whereas rivaroxaban pretreatment did not. The present study shows a lower risk of brain hemorrhage in rivaroxaban-pretreated compared to warfarin-pretreated rats following tPA administration to the ischemic brain. It is suggested that the relative down-regulation of PAR-1 and PAR-2 by rivaroxaban compared with warfarin pretreatment might be partly involved in the mechanism of reduced hemorrhagic complications in patients receiving rivaroxaban in clinical trials.

Significance

Several clinical trials have reported rivaroxaban, a direct FXa inhibitor, is superior to warfarin in terms of reducing intracerebral hemorrhage (ICH); however, the mechanism of ICH reduction by rivaroxaban is unclear. Some reports suggest that the effects of FXa are mediated by protease-activated receptors (PARs), and that activation of PARs contributes to neurodegeneration in neurological disorders. In an animal stroke model followed by tPA, we observed that warfarin pretreatment enhanced the expression of PAR-1 and PAR-2 in the brain, whereas rivaroxaban pretreatment did not. This result might be partly involved in the mechanism of reduced ICH in patients receiving rivaroxaban.

Introduction

Atrial fibrillation increases with age, causing cardiogenic embolic stroke to be the major cause of stroke among the elderly. Warfarin effectively prevents such cardioembolic stroke; however, there are several problems associated with warfarin use, such as its narrow therapeutic range that necessitates frequent blood monitoring, interactions with medications and foods, and increased risk of hemorrhage. The novel oral anticoagulant (NOAC) rivaroxaban is a direct activated factor X (FXa) inhibitor that is noninferior to warfarin for the prevention of stroke and is superior for bleeding side effects without blood monitoring (Patel et al., 2011). However, the mechanism of the greater reduction of intracerebral hemorrhage (ICH) by rivaroxaban compared with warfarin is unclear.

Recombinant tissue plasminogen activator (tPA) is established as the treatment of choice for acute ischemic stroke within 4.5 h of onset, but this treatment increases risk of symptomatic ICH for those taking oral anticoagulants with a prothrombin time–international normalized ratio (PT-INR) ≥ 1.7 , and even for those with a PT-INR < 1.7 (Seet et al., 2011; Shahjouei et al., 2015).

Protease-activated receptors (PARs) are G-protein–coupled receptors that are widely distributed in the brain. The PAR family consists of four members: PAR-1, PAR-2, PAR-3, and PAR-4. The effects of serine proteases, such as thrombin, FXa, and tPA are mediated by PARs. It has been reported that activation of PARs contributes to inflammation and neurodegeneration in many neurological disorders, including stroke (Steinhoff et al., 2005; Ossovskaya et al., 2004; Luo et al., 2007). However, there is no clear data for the safety of tPA in warfarin- or rivaroxaban-pretreated patients in relation to PAR activities.

Therefore, this study aimed to assess the risk of ICH after tPA treatment following rivaroxaban, warfarin or placebo pretreatment in relation to expression profiles of PAR-1, PAR-2, PAR-3, and PAR-4 in rat brain after stroke.

Materials and Methods

Animals

Male Wistar rats (11 weeks old, body weight 240-260 g; SLC, Shizuoka, Japan) were acclimatized to standard rat cages under conventional laboratory conditions with a 12/12 hour (h) light-dark cycle and constant humidity and room temperature of 23°C for 2 weeks. The animals were fed rat pellets (MF, Oriental Yeast, Tokyo, Japan). Water was provided *ad libitum* in bottles. One rat was kept in one cage and the cages were cleaned weekly, with paper pulp bedding (Oriental Yeast, Tokyo, Japan). All animal experiments complied with a protocol approved by the Animal Committee of the Graduate School of Medicine and Dentistry, Okayama University (OKU#2012675). The present study is a part of a stroke project, focusing on hemorrhagic complications, blood analysis, and inflammatory features such as immunoglobulin G (IgG) and PARs (clinical and other pathological aspects have been reported by Shang et al. [2016]).

Experimental groups and drug treatments

Rats were divided into four groups: vehicle-treated group (0.5% carboxymethyl cellulose sodium salt; V+tPA), warfarin pre-treated group (0.2 mg/kg/day; W+tPA), low dose rivaroxaban pre-treated group [60 mg/kg/day; R(L)+tPA], and high dose rivaroxaban pre-treated group [120 mg/kg/day; R(H)+tPA; Fig. 1]. The investigators who conducted the behavioral tests, operations, and immunohistochemistry analysis were blinded to the treatment assignment. Each drug was administered for 2 weeks, starting from when rats were 11 weeks old. Warfarin was administered orally once a day, and rivaroxaban was administered by chow diet. For each drug, the dose and interval between the last intake of drug and the induction of cerebral ischemia were determined to inhibit clot formation by

more than 70% in the rat venous thromboembolism model (Toomey et al., 2006; Perzborn et al., 2005; Kono et al., 2014) and a rivaroxaban PK experiment (Fig. 2). In the rivaroxaban PK experiment, 50 Wistar rats were fed ad libitum for 3 weeks with a basic pellet chow containing 600 or 1200 ppm rivaroxaban. Then the animals were anesthetized in groups of 5 animals at 5 daylight time points, and 5 mL of whole blood were collected from each animal (Fig. 2). We estimated each animal's body weight to be 250 g and daily food intake to be 25 g (containing 600 ppm or 1200 ppm rivaroxaban). A diet of 25 g/animal/day equates to a rivaroxaban dose of 60 or 120 mg/kg/day. We supplied the diet of 25 g/animal each day (one rat per cage) and watched whether the animals consumed all of the food supplied. We confirmed that most animals ate the full 25 g of food supplied each day.

One hour after the last administration of warfarin, blood was drawn from the left femoral vein. Prothrombin time (PT), activated partial thromboplastin time (aPTT), and the thrombin-antithrombin complex (TAT) were measured. In the vehicle and rivaroxaban groups, PT, aPTT, and TAT were measured at the same time of the warfarin group.

Focal Cerebral Ischemia

After 2 weeks of pretreatment, the rats were anesthetized with a mixture of nitrous oxide/oxygen/isoflurane (69%:30%:1%) using an inhalation mask. During the surgical procedure, body temperature was monitored and maintained at $37 \pm 0.3^{\circ}\text{C}$ using a heating pad. The right middle cerebral artery (MCA) was occluded by inserting a 4-0 surgical nylon thread with silicon coating through the common carotid artery as described previously (Abe et al., 1992). After 90 min of transient middle cerebral artery occlusion (tMCAO), the nylon thread was gently removed to restore blood flow in the MCA territory, and the rats were treated with tPA (Grtpa; Mitsubishi Tanabe Pharma Corporation, Osaka, Japan; intravenous bolus, 10 mg/kg per 10 mL). This relatively high dose of tPA was selected based on the report

of a tenfold difference in fibrin-specific activity between humans and rodents (Korninger and Collen, 1981). We calculated the sample size based on a report by Kono et al. (2014). To detect an increase in ICH with a two-sided 5% significance level and a power of 80%, a sample size of 30 rats per group was necessary, given an anticipated dropout rate of 50%. We used 121 rats in this study, of which 66 were excluded based on the following exclusion criteria: rats that died as a result of a procedural problem during surgery (n = 36), rats for which there were no neurological findings (n = 21), and rats that died after surgery in the period leading up to sacrifice (n = 9).

Tissue preparation

Twenty-four hours after reperfusion, the surviving rats (total n=55; 14 for the V+tPA group, 13 for the W+tPA group, 15 for the R(L)+tPA group, and 13 for R(H)+tPA group) were deeply anesthetized by intraperitoneal injection of pentobarbital (40 mg/kg) and transcardially perfused with ice-cold phosphate-buffered saline (PBS), and then ice-cold 4% paraformaldehyde (PFA) in 0.1 mol/L phosphate buffer. The whole brain was removed and immersed in the same fixative for 12 hours at 4°C. After washing with PBS, the tissues were sequentially transferred into 10, 20 and 30% (wt/vol) sucrose solutions and then embedded in powdered dry ice and stored at -80°C. 20- μ m-thick sections were prepared using a cryostat at -18°C and mounted on silane-coated glass slides.

Histology and single immunohistochemistry analysis

To determine the ischemic lesion area, brain sections were stained with hematoxylin-eosin and examined with a light microscope (Olympus BX-51; Olympus Optical, Tokyo, Japan). Sections were cut at 2, 0, -2, -4, and -6 mm from bregma. The infarct area was measured in these five sections by counting pixels using Photoshop CC, and the

infarct volume was calculated by multiplying the infarct area by 2 mm of thickness (Kawai et al., 2011). To analyze brain hemorrhage, iron staining was performed by an enhanced Perl reaction. Sections were incubated with Perl solution (5% potassium ferrocyanide and 5% HCl; 1:1) for 45 min, washed in distilled water, and incubated again in 0.5% diamine benzidine tetrahydrochloride with nickel for 60 min (Wu et al., 2003).

It has been reported that endogenous rat IgG is immunolocalized in areas of blood-brain barrier (BBB) breakdown (Richmon et al., 1998). To estimate levels of rat IgG, sections were incubated with biotin-labeled rabbit anti-rat IgG antibody (1:500; Vector Laboratories, BA-4000, AB_2336206). Immunoreactivities were developed in horseradish peroxidase streptavidin-biotin complex solution (Vectastain ABC kit; Vector Laboratories, PK-6104, AB_2336206) and then incubated with diaminobenzidine tetrahydrochloride.

For further immunohistochemistry, we used the following primary antibodies. All antibodies used in this study were from commercial sources (see Table I): mouse anti-PAR-1 antibody (1:50; Santa Cruz Biotechnology, Santa Cruz, CA, USA, sc-13503, AB_2101175), mouse anti-PAR-2 antibody (1:50; Santa Cruz Biotechnology, sc-13504, AB_628101), goat anti-PAR-3 antibody (1:50; Santa Cruz Biotechnology, sc-8209, AB_2101327), goat anti-PAR-4 antibody (1:50; Santa Cruz Biotechnology, sc-8462, AB_2159244), rabbit anti-neuronal nuclei (NeuN) antibody (1:500; Abcam, Cambridge, UK, ab104225, AB_10711153); biotinylated lycopersicon esculentum lectin (LEL) (1:200; Vector Laboratories, Burlingame, CA, USA, B-1175, AB_2315475); rabbit anti-glutathione S-transferase pi-1 (GST- π) antibody (1:500; MBL, Woburn, MA, USA, 312, AB_591792); rabbit anti-gial fibrillary acidic protein (GFAP) antibody (1:1000; Dako, Carpinteria, CA, USA, Z0334, AB_10013382) and rabbit anti-ionized calcium binding adaptor molecule-1 (Iba-1) antibody (1:1000; Wako Chemicals, Richmond, VA, USA, 019-19741, AB_839504). LEL is a glycoprotein with affinity for NAGO, which is expressed by mature vascular

endothelial cells (Augustin et al., 1995). To estimate the expression levels of PAR-1, PAR-2, PAR-3, and PAR-4, sections were incubated with the respective first antibody and then incubated with an appropriate biotin-labeled secondary antibody (1:500, Vector Laboratories).

Double immunofluorescence analysis

To determine the localization of PARs in the peri-ischemic lesion, double immunofluorescence studies were performed for PARs (PAR-1, PAR-2, PAR-3, and PAR-4) plus NeuN, NAGO, GST- π , GFAP, and Iba-1. Immunoreactivities were visualized using appropriate fluorescent secondary antibody, that is, donkey anti-goat IgG antibody conjugated with Alexa 555 (Thermo Fisher Scientific, A21432, RRID:AB_10053826), goat anti-mouse IgG antibody conjugated with Alexa 555 (Thermo Fisher Scientific, A21424, RRID:AB_10566287), donkey anti-rabbit IgG antibody conjugated with Alexa 488 (Thermo Fisher Scientific, A21206, RRID:AB_10049650), chicken anti-rabbit IgG antibody conjugated with FITC (Millipore, AP169F, RRID:AB_92561), and fluorescein FITC antibody (Vector Laboratories, A-2001, RRID:AB_2336455). The treated sections were scanned and captured at $\times 100$ magnification for the confocal microscopy equipped with an argon and HeNe1 laser (LSM-510; Zeiss, Jena, Germany).

Semiquantitative analysis

For the semiquantitative evaluation of rat IgG and PAR (PAR-1, 2, 3, 4) staining intensity, stained sections of the caudate putamen (1.2, 0.7, and 0.2 mm rostral to the bregma) (Paxinos and Watson, 1982) were selected from each rat, and three areas in the ipsilateral peri-infarcted cortex and contralateral cortex in each section were chosen randomly and captured $\times 200$ magnification for the light microscopy. Staining intensity was measured with image processing software (Scion Image, Scion Corporation, Frederick, MD, USA).

Statistical analysis

Data were analyzed in SPSS v.22.0 (IBM, Armonk, NY). All data are expressed as the mean \pm SE. Between-subjects ANOVA was used to identify difference among peri-ischemic lesion and contralateral hemisphere. One-way analysis of ANOVA was used to compare the four groups (V+tPA, W+tPA, R(L)+tPA, and R(H)+tPA) followed by a Tukey's honestly significant difference test for normally distributed data. Non-normally distributed data were evaluated using the Kruskal–Wallis variance analysis test followed by the Ryan-corrected Mann–Whitney U test. A $p < 0.05$ was considered statistically significant.

Results

Infarct volume, intracerebral hemorrhage, and IgG leakage

Survival rates 24 h after surgery of the V+tPA, W+tPA, R(L)+tPA, and R(H)+tPA groups were 93.3% ($n = 14$), 76.5% ($n = 13$), 88.2% ($n = 15$), and 86.7% ($n = 13$), respectively (Fig. 3A), and infarct volumes did not differ among the four groups ($F_{3,51} = 0.49$; $n = 55$; $p = 0.69$, one-way ANOVA; Fig. 3B). However, greater ICH was observed in the W+tPA group compared with the R(L)+tPA and R(H)+tPA groups (Fig. 3C). This difference was confirmed by quantification; the ICH volume was significantly larger in the W+tPA group than in the V+tPA or R(L)+tPA or R(H)+tPA groups (total $n = 55$; $p < 0.001$, Ryan-corrected Mann–Whitney U test; Fig. 3D).

BBB break-down leads to endogenous rat IgG leaking from blood vessels into brain parenchyma (Richmon et al., 1998). The W+tPA group showed a stronger IgG staining within neurons and neuropil, but the differences were not significant among the four groups ($H = 4.17$; $n = 55$; $p = 0.24$, Kruskal–Wallis test; Fig. 3E-F).

Blood Analysis

Just before tMCAO, PT was significantly prolonged in the W+tPA and R(H)+tPA groups compared with the V+tPA group (Total n = 42; $p < 0.001$, Ryan-corrected Mann–Whitney U test; Fig. 4A). aPTT was not different among the four groups ($F_{3,33} = 0.92$; n = 37; $p = 0.65$, one-way ANOVA; Fig. 4B). Although TAT was significantly reduced in the W+tPA ($p = 0.009$), R(L)+tPA ($p = 0.012$), and R(H)+tPA ($p = 0.008$) groups compared with the V+tPA group (total n = 46, Turkey's test; Fig. 4C), there was no difference among the W+tPA, R(L)+tPA, and R(H)+tPA groups. This result supports anticoagulant levels being the same among the three drug groups.

Immunoreactivity for PAR 1-4

PAR-1, PAR-2, PAR-3, and PAR-4 were widely but weakly expressed in the normal brain. PAR-1, PAR-2, PAR-3, and PAR-4 were widely but weakly expressed in the normal brain. Their levels, assessed by pixel intensity, were increased in the ischemic brain, especially in the peri-ischemic lesion ($F = 10.4–121.3$, $p = 0.001–0.05$, between-subjects ANOVA; Fig. 5B–E).

In the V+tPA group, PAR-1 and PAR-2 immunoreactivities were mainly detected in neurons (Fig. 5A, a, b) and weakly detected in blood vessels of the peri-ischemic lesion (Fig. 5A, a, b, insets). PAR-3 immunoreactivity was found in both neurons (Fig. 5A, c) and blood vessels (Fig. 5A, c, inset). PAR-4 was observed only in neurons (Fig. 5A, d). Compared to the V+tPA group, the number and the pixel intensity of PAR-1 were significantly increased in the W+tPA group in the peri-ischemic lesion ($p = 0.030$, $p = 0.020$, respectively), and this increase was not observed by low dose rivaroxaban treatment ($p = 0.021$, $p = 0.012$, respectively, Turkey's test; Fig. 5A-B). The pixel intensity of PAR-2 in the W+tPA group in the peri-ischemic lesion was increased ($p < 0.001$) similarly to that of PAR-1, and this

increase was also not observed by low dose rivaroxaban treatment ($p = 0.004$, Ryan-corrected Mann–Whitney U test; Fig. 5A, C). In addition, the pixel intensity of PAR-2 in the contralateral hemisphere was less in the R(L)+tPA group compared to the W+tPA group ($p = 0.006$, Ryan-corrected Mann–Whitney U test; Fig. 5C). The number of PAR-3-positive cells in the contralateral hemisphere was decreased in the R(L)+tPA and R(H)+tPA groups compared to the W+tPA group ($p < 0.001$, $p = 0.003$, respectively, Ryan-corrected Mann–Whitney U test; Fig. 5D), but there was no significant difference in the peri-ischemic lesion ($F_{3,51}=0.50$; $n = 55$; $p=0.69$, one-way ANOVA; Fig. 5D). In contrast, there was no significant difference in the number and density of PAR-4 pixels in both the peri-ischemic lesion and the contralateral hemisphere ($H = 0.94-5.08$; $n = 55$, $p = 0.17-0.82$, Kruskal–Wallis test; Fig. 5E).

Double immunostaining for PAR 1-4 in the peri-ischemic lesion

A double immunofluorescence study of the V+tPA group showed that PAR-1 colocalized with some NeuN-positive neurons (Fig. 6a, arrows). PAR-1 generally did not colocalize with NAGO-positive vascular endothelial cells, but a small amount of PAR-1 immunoreactivity was localized adjacent to endothelial cells (Fig. 6b, inset, arrowhead). On the other hand, PAR-1 did not colocalize with GST-positive oligodendrocytes (Fig. 6c), GFAP-positive astrocytes (Fig. 6d), or Iba-1-positive microglia (Fig. 6e). PAR-2 also colocalized with some neurons (Fig. 6f, arrows), and was distributed adjacent to a small number of endothelial cells (Fig. 6g). Similar to PAR-1, PAR-2 did not colocalize with oligodendrocytes (Fig. 6h), astrocytes (Fig. 6i), or microglia (Fig. 6j). Unlike PAR-1 and PAR-2, PAR3 strongly colocalized both with neurons (Fig. 6k, arrows) and vascular endothelial cells (Fig. 6l, arrows), but again did not colocalize with oligodendrocytes (Fig. 6m), astrocytes (Fig. 6n), or microglia (Fig. 6o). PAR-4 colocalized only with some neurons (Fig. 6p, arrows), but not with vascular endothelial cells (Fig. 6q), oligodendrocytes (Fig. 6r), astrocytes (Fig. 6s), or

microglia (Fig. 6t).

Double immunofluorescence studies of the W+tPA, R(L)+tPA, and R(H)+tPA groups showed the same pattern as the V+tPA group, but the expression levels of PAR-1 and PAR-2 were stronger in the W+tPA group, and suppressed in the R(L)+tPA group (data not shown).

Discussion

In the present study, the severity of brain hemorrhage was increased (Fig. 3D-E) and IgG leakage tended to increase (Fig. 3E-F) in ischemia rats following tPA administration pretreated with warfarin but not with rivaroxaban. These results are similar to our previous reports which shows a lower risk of intracerebral hemorrhage in the dabigatran or apixaban-pretreated treated groups compared with the warfarin-treated group (Kono et al., 2014a, 2014b). PAR-1, PAR-2, PAR-3, and PAR-4 were widely distributed in the contralateral non-ischemic side, and their levels were significantly upregulated in the ischemic side (Fig. 5B-E). We observed that warfarin pretreatment enhanced the expression of PAR-1 and PAR-2 in the peri-ischemic lesion; however, rivaroxaban pretreatment did not (Fig. 5A-C).

PAR-1 expression in the brain

PAR-1 is widely expressed in the brain, including neurons (Striggow et al., 2001; Wang J et al., 2012), vascular endothelial cells (Bartha et al., 2000; Nelken et al., 1992), oligodendrocytes (Wang Y et al., 2004), astrocytes (Pompili et al., 2004; Wang H et al., 2002), and microglia (Henrich-Noack et al., 2006; Pompili et al., 2011; Balcaitis et al., 2003). However, in the present study, double staining showed PAR-1 to be mainly localized in neurons and to be present at low levels in vascular endothelial cells (Fig. 5A, 6a-b), but not colocalized with GST- π (oligodendrocytes), GFAP (astrocytes), or Iba-1 (microglia) (Fig.

6c-e). A PAR-1 agonist increases brain infarct volume after cerebral ischemia, triggering astrogliosis (Nicole et al., 2005), activating microglia (Suo et al., 2002), and increasing mRNA expression of IL-6, IL-1 β , and TNF- α (Fan et al., 2005), which was absent in mice lacking PAR-1 (Wang J et al., 2012; Junge et al., 2003; Rajput et al., 2014; Olson et al., 2004). In the present study, warfarin pretreatment enhanced the expression of PAR-1 in the peri-ischemic lesion (Fig. 5A-B).

PAR-2 expression in the brain

PAR-2 is also widely expressed in the *in vivo* brain, including in neurons (Suo et al., 2002), astrocytes (Pompili et al., 2004; Jin et al., 2005; Noorbakhsh et al., 2006), and microglia (Noorbakhsh et al., 2006), but has only been observed to be expressed in vascular endothelial cells cultured *in vitro* (Bartha et al., 2000). In the present study, however, we did observe PAR-2 expression in vascular endothelial cells of the *in vivo* rat brain (Fig. 6g). We previously reported that expression of PAR-2 is enhanced after cerebral ischemia in mice, and that genetic deletion of PAR-2 increased the infarct volume and brain damage (Jin et al., 2005). PAR-2 has either neuroprotective or neurodegenerative effects depending on the levels of expression and the cell type (Bushell, 2007). Here, we found that warfarin pretreatment enhanced the expression of PAR-2 (Fig. 5A, C).

Rivaroxaban could be associated with the PAR-1 and PAR-2 activities

The current study is the latter part of a larger stroke project and in our previous report (Shang et al., 2016) we found upregulation of matrix metalloproteinase-9 (MMP-9) and a marked dissociation of the neurovascular unit (NVU) in the W+tPA group, which was ameliorated by replacing warfarin with rivaroxaban. Many reports suggest that FXa influences various molecular effects by activating PAR-1 and PAR-2 (Steinhoff et al., 2005;

Ossovskaya et al; 2004; Luo et al., 2007), and rivaroxaban prevents FXa-induced PAR-1 and PAR-2 activities, which leads to attenuation of inflammation (Hara et al., 2015; Sparkenbaugh et al., 2014; Bukowska et al., 2013). In the present study, the enhanced PAR-1 and PAR-2 expression found in the warfarin group was largely not produced by rivaroxaban treatment (Fig. 5A-C). The attenuations of MMP-9 activity, NVU dissociation (Shang et al., 2016), brain hemorrhage (Fig. 3C-D), and IgG leakage (Fig. 3E-F) by rivaroxaban treatment could be associated with the suppression of PAR-1 and PAR-2 activities.

PAR-3 and PAR-4 expressions in the brain

PAR-3 is involved in thrombin signaling in mice platelets as a cofactor for the cleavage and activation of PAR-4 (Nakanishi-Matsui et al., 2000). Several reports have demonstrated PAR-3 to be distributed in the brain, including in neurons (Striggow et al., 2001), vascular endothelial cells (Bartha et al., 2000), astrocytes (Pompili et al., 2004; Wang H et al., 2002), and microglia (Henrich-Noack et al., 2006). We observed PAR-3 upregulation both in neurons and blood vessels in the post-ischemic rat brain (Fig. 5D), suggesting that PAR-3 is involved in ischemic brain injury or the repair process both through neuronal and vascular endothelial mechanisms after cerebral ischemia.

PAR-4 is a key regulator of coagulation and inflammation under pathological conditions (Suo et al., 2003; French and Hamilton, 2016). PAR-4-deficient mice show infarct volume reduction, suggesting a neurodegenerative effect and inflammatory aggravating effects (Mao et al., 2010). Similar to a previous report (Henrich-Noack et al., 2006), PAR-4 levels were increased in the ischemic brain (Fig. 5E), but there was no difference in PAR-4 expression between the groups receiving warfarin and rivaroxaban (Fig. 5E).

There is a limitation to the present study. With respect to upregulation of PARs and increase in ICH, it is difficult to differentiate between cause and effect. Warfarin pretreatment

can cause MMP-9 upregulation and NVU disruption (see our previous report, Shang J, et al. 2016); we speculate that this may lead to enhancement of inflammation and upregulation of PARs. These increases in inflammation and PAR levels may further accelerate NVU dissociation and ICH. In future research, we intend to use pharmacological approaches and transgenic animals to address this question.

Conclusion

In summary, the present study suggests a lower risk of brain hemorrhage in rats pretreated with rivaroxaban after brain ischemia and tPA administration compared with pretreatment with warfarin. Warfarin-induced upregulation of PAR-1 and PAR-2 was not observed with rivaroxaban pretreatment, suggesting that activation of PAR-1 and PAR-2 might be associated with brain injury, such as BBB break-down and ICH after tPA. In contrast, there were no differences in expression levels of PAR-3 and PAR-4 between warfarin- and rivaroxaban-treated rats. It is suggested that these results might be partly involved in the mechanism of reduced hemorrhagic complications in patients receiving rivaroxaban in the ROCKET-AF trial (Patel et al., 2011).

Conflict of Interest

This work was mainly supported by Bayer Yakuhin, Ltd.

Role of Authors

All authors had full access to all the data in the study and take responsibility for the integrity of the data and the accuracy of the data analysis. Study concept and design: KA. Acquisition of data: RM, SK, SH, EP. Analysis and interpretation of data: RM, SK, SH, EP. Drafting of the manuscript: RM. Critical revision of the manuscript for important intellectual

content: TY, YN, KS, NH, YO, SH, KA. Statistical analysis: RM. Obtained funding: KA. Administrative, technical, and material support: RM, SK, JS, SH, EP. Study supervision: KA.

Data Accessibility

We provide a small amount of additional data as a Supplementary file.

References

- Abe K, Kawagoe J, Araki T, Aoki M, Kogure K. 1992. Differential expression of heat shock protein 70 gene between the cortex and caudate after transient focal cerebral ischaemia in rats. *Neurol Res* 14:381-385.
- Augustin HG, Braun K, Telemenakis I, Modlich U, Kuhn W. 1995. Ovarian angiogenesis. Phenotypic characterization of endothelial cells in a physiological model of blood vessel growth and regression. *Am J Pathol* 147:339-351.
- Balcaitis S, Xie Y, Weinstein JR, Andersen H, Hanisch UK, Ransom BR, Moller T. 2003. Expression of proteinase-activated receptors in mouse microglial cells. *Neuroreport* 14:2373-2377.
- Bartha K, Domotor E, Lanza F, Adam-Vizi V, Machovich R. 2000. Identification of thrombin receptors in rat brain capillary endothelial cells. *J Cereb Blood Flow Metab* 20:175-182.
- Bukowska A, Zacharias I, Weinert S, Skopp K, Hartmann C, Huth C, Goette A. 2013. Coagulation factor Xa induces an inflammatory signalling by activation of protease-activated receptors in human atrial tissue. *Eur J Pharmacol* 718:114-123.
- Bushell T. 2007. The emergence of proteinase-activated receptor-2 as a novel target for the treatment of inflammation-related CNS disorders. *J Physiol* 581:7-16.
- Fan Y, Zhang W, Mulholland M. 2005. Thrombin and PAR-1-AP increase proinflammatory cytokine expression in C6 cells. *J Surg Res* 129:196-201.

- French SL, Hamilton JR. 2016. Protease-activated receptor 4: from structure to function and back again. *Br J Pharmacol*.
- Hara T, Fukuda D, Tanaka K, Higashikuni Y, Hirata Y, Nishimoto S, Yagi S, Yamada H, Soeki T, Wakatsuki T, Shimabukuro M, Sata M. 2015. Rivaroxaban, a novel oral anticoagulant, attenuates atherosclerotic plaque progression and destabilization in ApoE-deficient mice. *Atherosclerosis* 242:639-646.
- Henrich-Noack P, Riek-Burchardt M, Baldauf K, Reiser G, Reymann KG. 2006. Focal ischemia induces expression of protease-activated receptor1 (PAR1) and PAR3 on microglia and enhances PAR4 labeling in the penumbra. *Brain Res* 1070:232-241.
- Jin G, Hayashi T, Kawagoe J, Takizawa T, Nagata T, Nagano I, Syoji M, Abe K. 2005. Deficiency of PAR-2 gene increases acute focal ischemic brain injury. *J Cereb Blood Flow Metab* 25:302-313.
- Junge CE, Sugawara T, Mannaioni G, Alagarsamy S, Conn PJ, Brat DJ, Chan PH, Traynelis SF. 2003. The contribution of protease-activated receptor 1 to neuronal damage caused by transient focal cerebral ischemia. *Proc Natl Acad Sci U S A* 100:13019-13024.
- Kataoka H, Hamilton JR, McKemy DD, Camerer E, Zheng YW, Cheng A, Griffin C, Coughlin SR. 2003. Protease-activated receptors 1 and 4 mediate thrombin signaling in endothelial cells. *Blood* 102:3224-3231.
- Kawai H, Deguchi S, Deguchi K, Yamashita T, Ohta Y, Shang J, Tian F, Zhang X, Liu N, Liu W, Ikeda Y, Matsuura T, Abe K. 2011. Synergistic benefit of combined amlodipine plus atorvastatin on neuronal damage after stroke in Zucker metabolic rat. *Brain Res* 1368:317-323.
- Kono S, Deguchi K, Omote Y, Yunoki T, Yamashita T, Kurata T, Ikeda Y, Abe K. 2014. Reducing hemorrhagic complication by dabigatran via neurovascular protection after recanalization with tissue plasminogen activator in ischemic stroke of rat. *J Neurosci Res*

92:46-53.

- Kono S, Yamashita T, Deguchi K, Omote Y, Yunoki T, Sato K, Kurata T, Hishikawa N, Abe K. 2014. Rivaroxaban and apixaban reduce hemorrhagic transformation after thrombolysis by protection of neurovascular unit in rat. *Stroke* 45:2404-2410.
- Korninger C, Collen D. 1981. Studies on the specific fibrinolytic effect of human extrinsic (tissue-type) plasminogen activator in human blood and in various animal species in vitro. *Thrombosis and haemostasis* 46:561-565.
- Luo W, Wang Y, Reiser G. 2007. Protease-activated receptors in the brain: receptor expression, activation, and functions in neurodegeneration and neuroprotection. *Brain Res Rev* 56:331-345.
- Mao Y, Zhang M, Tuma RF, Kunapuli SP. 2010. Deficiency of PAR4 attenuates cerebral ischemia/reperfusion injury in mice. *J Cereb Blood Flow Metab* 30:1044-1052.
- Nakanishi-Matsui M, Zheng YW, Sulciner DJ, Weiss EJ, Ludeman MJ, Coughlin SR. 2000. PAR3 is a cofactor for PAR4 activation by thrombin. *Nature* 404:609-613.
- Nelken NA, Soifer SJ, O'Keefe J, Vu TK, Charo IF, Coughlin SR. 1992. Thrombin receptor expression in normal and atherosclerotic human arteries. *J Clin Invest* 90:1614-1621.
- Nicole O, Goldshmidt A, Hamill CE, Sorensen SD, Sastre A, Lyuboslavsky P, Hepler JR, McKeon RJ, Traynelis SF. 2005. Activation of protease-activated receptor-1 triggers astrogliosis after brain injury. *J Neurosci* 25:4319-4329.
- Noorbakhsh F, Tsutsui S, Vergnolle N, Boven LA, Shariat N, Vodjgani M, Warren KG, Andrade-Gordon P, Hollenberg MD, Power C. 2006. Proteinase-activated receptor 2 modulates neuroinflammation in experimental autoimmune encephalomyelitis and multiple sclerosis. *J Exp Med* 203:425-435.
- Olson EE, Lyuboslavsky P, Traynelis SF, McKeon RJ. 2004. PAR-1 deficiency protects against neuronal damage and neurologic deficits after unilateral cerebral hypoxia/ischemia.

- J Cereb Blood Flow Metab 24:964-971.
- Ossovskaya VS, Bunnett NW. 2004. Protease-activated receptors: contribution to physiology and disease. *Physiol Rev* 84:579-621.
- Patel MR, Mahaffey KW, Garg J, Pan G, Singer DE, Hacke W, Breithardt G, Halperin JL, Hankey GJ, Piccini JP, Becker RC, Nessel CC, Paolini JF, Berkowitz SD, Fox KA, Califf RM. 2011. Rivaroxaban versus warfarin in nonvalvular atrial fibrillation. *N Engl J Med* 365:883-891.
- Paxinos G, Watson C. *The rat brain in stereotaxic coordinates*. New York, NY: Academic Press; 1982.
- Perzborn E, Strassburger J, Wilmen A, Pohlmann J, Roehrig S, Schlemmer KH, Straub A. 2005. In vitro and in vivo studies of the novel antithrombotic agent BAY 59-7939--an oral, direct Factor Xa inhibitor. *J Thromb Haemost* 3:514-521.
- Pompili E, Fabrizi C, Nori SL, Panetta B, Geloso MC, Corvino V, Michetti F, Fumagalli L. 2011. Protease-activated receptor-1 expression in rat microglia after trimethyltin treatment. *J Histochem Cytochem* 59:302-311.
- Pompili E, Nori SL, Geloso MC, Guadagni E, Corvino V, Michetti F, Fumagalli L. 2004. Trimethyltin-induced differential expression of PAR subtypes in reactive astrocytes of the rat hippocampus. *Brain Res Mol Brain Res* 122:93-98.
- Rajput PS, Lyden PD, Chen B, Lamb JA, Pereira B, Lamb A, Zhao L, Lei IF, Bai J. 2014. Protease activated receptor-1 mediates cytotoxicity during ischemia using in vivo and in vitro models. *Neuroscience* 281c:229-240.
- Richmon JD, Fukuda K, Maida N, Sato M, Bergeron M, Sharp FR, Panter SS, Noble LJ. 1998. Induction of heme oxygenase-1 after hyperosmotic opening of the blood-brain barrier. *Brain Res* 780:108-118.
- Seet RC, Zhang Y, Moore SA, Wijedicks EF, Rabinstein AA. 2011. Subtherapeutic

international normalized ratio in warfarin-treated patients increases the risk for symptomatic intracerebral hemorrhage after intravenous thrombolysis. *Stroke* 42:2333-2335.

Shahjouei S, Tsivgoulis G, Bavarsad Shahripour R, Jones GM, Alexandrov AV, Zand R. 2015. Safety of Intravenous Thrombolysis among Stroke Patients Taking New Oral Anticoagulants--Case Series and Systematic Review of Reported Cases. *Journal of stroke and cerebrovascular diseases : the official journal of National Stroke Association* 24:2685-2693.

Shang J, Yamashita T, Kono S, Morihara R, Nakano Y, Fukui Y, Li X, Hishikawa N, Ohta Y, Abe K. 2016. Effects of Pretreatment with Warfarin or Rivaroxaban on Neurovascular Unit Dissociation after Tissue Plasminogen Activator Thrombolysis in Ischemic Rat Brain. *J Stroke Cerebrovasc Dis.* 25:1997-2003

Soifer SJ, Peters KG, O'Keefe J, Coughlin SR. 1994. Disparate temporal expression of the prothrombin and thrombin receptor genes during mouse development. *Am J Pathol* 144:60-69.

Sparkenbaugh EM, Chantrathammachart P, Mickelson J, van Ryn J, Hebbel RP, Monroe DM, Mackman N, Key NS, Pawlinski R. 2014. Differential contribution of FXa and thrombin to vascular inflammation in a mouse model of sickle cell disease. *Blood* 123:1747-1756.

Steinhoff M, Buddenkotte J, Shpacovitch V, Rattenholl A, Moormann C, Vergnolle N, Luger TA, Hollenberg MD. 2005. Proteinase-activated receptors: transducers of proteinase-mediated signaling in inflammation and immune response. *Endocr Rev* 26:1-43.

Strigow F, Riek-Burchardt M, Kiesel A, Schmidt W, Henrich-Noack P, Breder J, Krug M, Reymann KG, Reiser G. 2001. Four different types of protease-activated receptors are widely expressed in the brain and are up-regulated in hippocampus by severe ischemia. *Eur J Neurosci* 14:595-608.

- Suo Z, Wu M, Ameenuddin S, Anderson HE, Zoloty JE, Citron BA, Andrade-Gordon P, Festoff BW. 2002. Participation of protease-activated receptor-1 in thrombin-induced microglial activation. *J Neurochem* 80:655-666.
- Suo Z, Wu M, Citron BA, Gao C, Festoff BW. 2003. Persistent protease-activated receptor 4 signaling mediates thrombin-induced microglial activation. *J Biol Chem* 278:31177-31183.
- Toomey JR, Abboud MA, Valocik RE, Koster PF, Burns-Kurtis CL, Pillarisetti K, Danoff TM, Erhardt JA. 2006. A comparison of the beta-D-xyloside, odiparcil, to warfarin in a rat model of venous thrombosis. *J Thromb Haemost* 4:1989-1996.
- Wang H, Ubl JJ, Reiser G. 2002. Four subtypes of protease-activated receptors, co-expressed in rat astrocytes, evoke different physiological signaling. *Glia* 37:53-63.
- Wang J, Jin H, Hua Y, Keep RF, Xi G. 2012. Role of protease-activated receptor-1 in brain injury after experimental global cerebral ischemia. *Stroke* 43:2476-2482.
- Wang Y, Richter-Landsberg C, Reiser G. 2004. Expression of protease-activated receptors (PARs) in OLN-93 oligodendroglial cells and mechanism of PAR-1-induced calcium signaling. *Neuroscience* 126:69-82.
- Wu J, Hua Y, Keep RF, Nakamura T, Hoff JT, Xi G. 2003. Iron and iron-handling proteins in the brain after intracerebral hemorrhage. *Stroke* 34:2964-2969.

Figure Legends

Figure 1. Experimental groups including the vehicle-treated (V+tPA) group, warfarin-treated (W+tPA) group, low dose rivaroxaban-treated [R(L)+tPA] group, and high dose rivaroxaban-treated [R(H)+tPA] group. At 24 h after 1.5 h of transient middle cerebral artery occlusion (tMCAO) followed by tissue plasminogen activator (tPA) administration, rats were sacrificed. p.o., per os.

Figure 2. 50 Wistar rats were fed with chow containing rivaroxaban for 3 weeks, and 5mL blood was drawn and treated with citrate. Rivaroxaban plasma levels (measured during the 12 h light period) of about 0.3-0.7 mg/L at low dose and 0.8-1.5 mg/L at high dose were achieved.

Figure 3. Survival rates (**A**) and infarction volume (**B**) were not different among the 4 groups. (**C**) Representative photographs of intracerebral hemorrhage (ICH) showing strong and weak ICH in the W+tPA group (arrows), and R(L)+tPA and R(H)+tPA groups, respectively. Scale bar: 2 mm. (**D**) Quantification of ICH volume. (**E** and **F**) The W+tPA group showed stronger IgG staining within neurons and neuropil, but the differences were not significant among the four groups. Scale bar: 50 μ m. $**p < 0.01$ vs V+tPA, $### p < 0.01$ vs W+tPA.

Figure 4. Blood analysis in the four groups, showing (**A**) significant prothrombin time (PT) prolongation in the W+tPA and R(H)+tPA groups, (**B**) no difference of the activated PT (aPTT) among the four groups, and (**C**) significant reduction of thrombin-antithrombin complex (TAT) in the W+tPA, R(L)+tPA, and R(H)+tPA groups. $*p < 0.05$; $**p < 0.01$ vs V+tPA.

Figure 5. Representative photomicrographs of protease-activated receptor-1, -2, -3, and -4 (PAR-1, PAR-2, PAR-3, PAR-4) staining in the peri-ischemic lesion (**A**) and the number and pixel intensity of PAR-1 (**B**), PAR-2 (**C**), PAR-3 (**D**), and PAR-4 (**E**) in the peri-ischemic lesion and contralateral hemisphere. Note that PAR-1 (**a, e, i, m**) and PAR-2 (**b, f, j, m**) were mainly detected in neurons and weakly detected in blood vessels (**insets**). PAR-3 (**c, g, k, o**) was found in both neurons and blood vessels (**insets**), and PAR-4 was observed only in neurons (**d, h, l, p**). The number and pixel intensity of PAR-1 (**B**) and PAR-2 (**C**) was increased in the W+tPA group in peri-ischemic lesions ($*p < 0.05$, vs V+tPA), but not by low dose rivaroxaban treatment. In contrast, no such difference was observed for PAR-3 and PAR-4 (**D, E**). Scale bar: 30 μm . $*p < 0.05$; $**p < 0.01$ vs V+tPA, $\# p < 0.05$; $\#\# p < 0.01$ vs W+tPA.

Figure 6. Double immunostaining for PAR 1-4 with neuronal nuclei (NeuN; **a, f, k, p**), N-acetylglucosamine oligomers (NAGO; **b, g, l, q**), glutathione S-transferase pi-1 (GST- π ; **c, h, m, r**), glial fibrillary acidic protein (GFAP; **d, i, n, s**), and ionized calcium binding adaptor molecule-1 (Iba-1; **e, j, o, t**) in peri-ischemic lesions of the V+tPA group. The PAR-1-positive cells are mainly colocalized with NeuN (**a, arrow**) and a small number with NAGO (**b, inset, arrowhead**), with no colocalization was observed with GST- π (**c**), GFAP (**d**), or Iba-1 (**e**). PAR-2-positive cells are also colocalized with NeuN (**f, arrow**) and a small number with NAGO (**g, inset, arrowhead**). PAR-3 was strongly colocalized with both NeuN (**k, arrows**) and NAGO (**l, arrows**), but not with GST- π (**m**), GFAP (**n**), or Iba-1 (**o**). PAR-4 only colocalized with NeuN (**p, arrows**). Scale bar: 20 μm .

Fig 6.

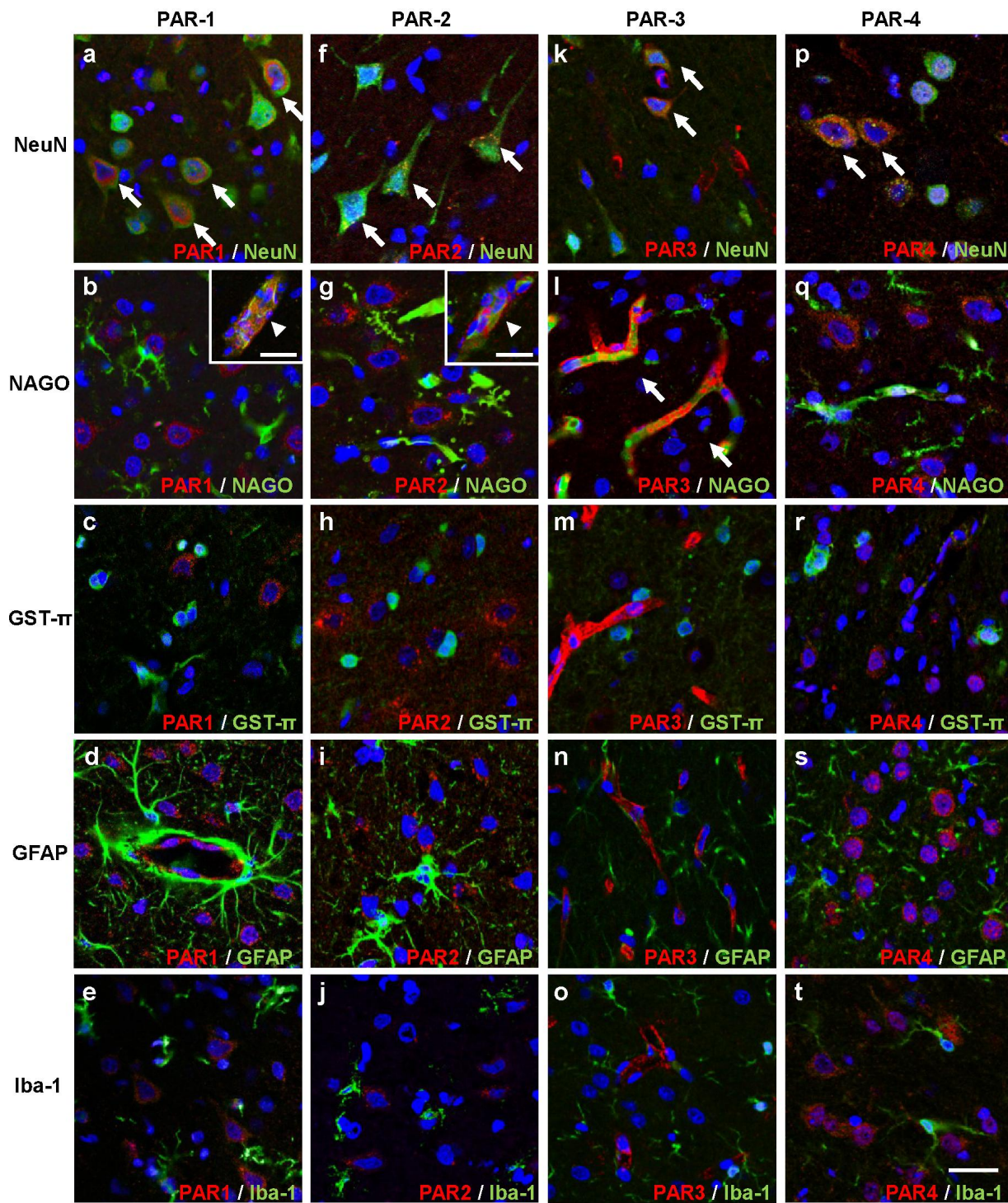


Fig 1.

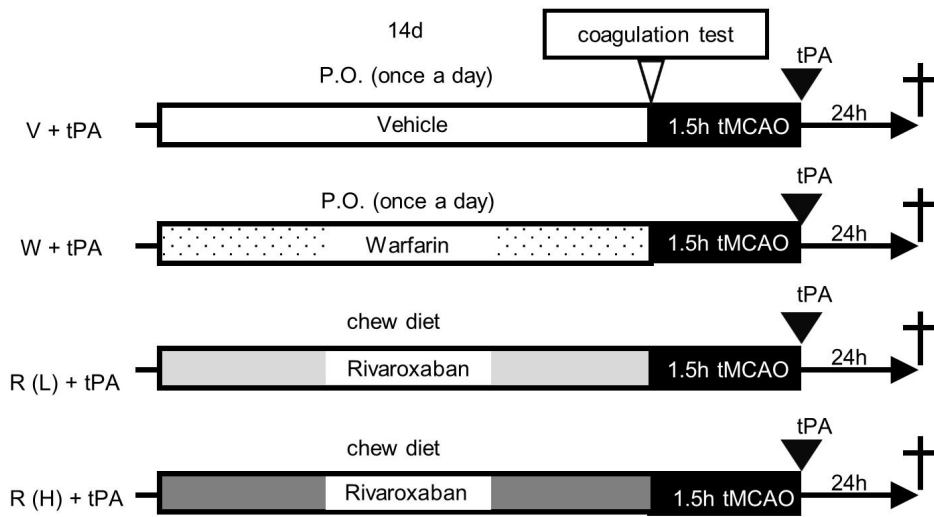


Fig 2.

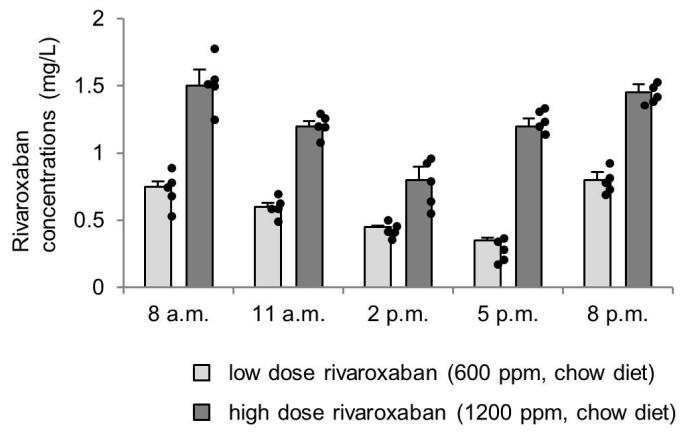


Fig 3.

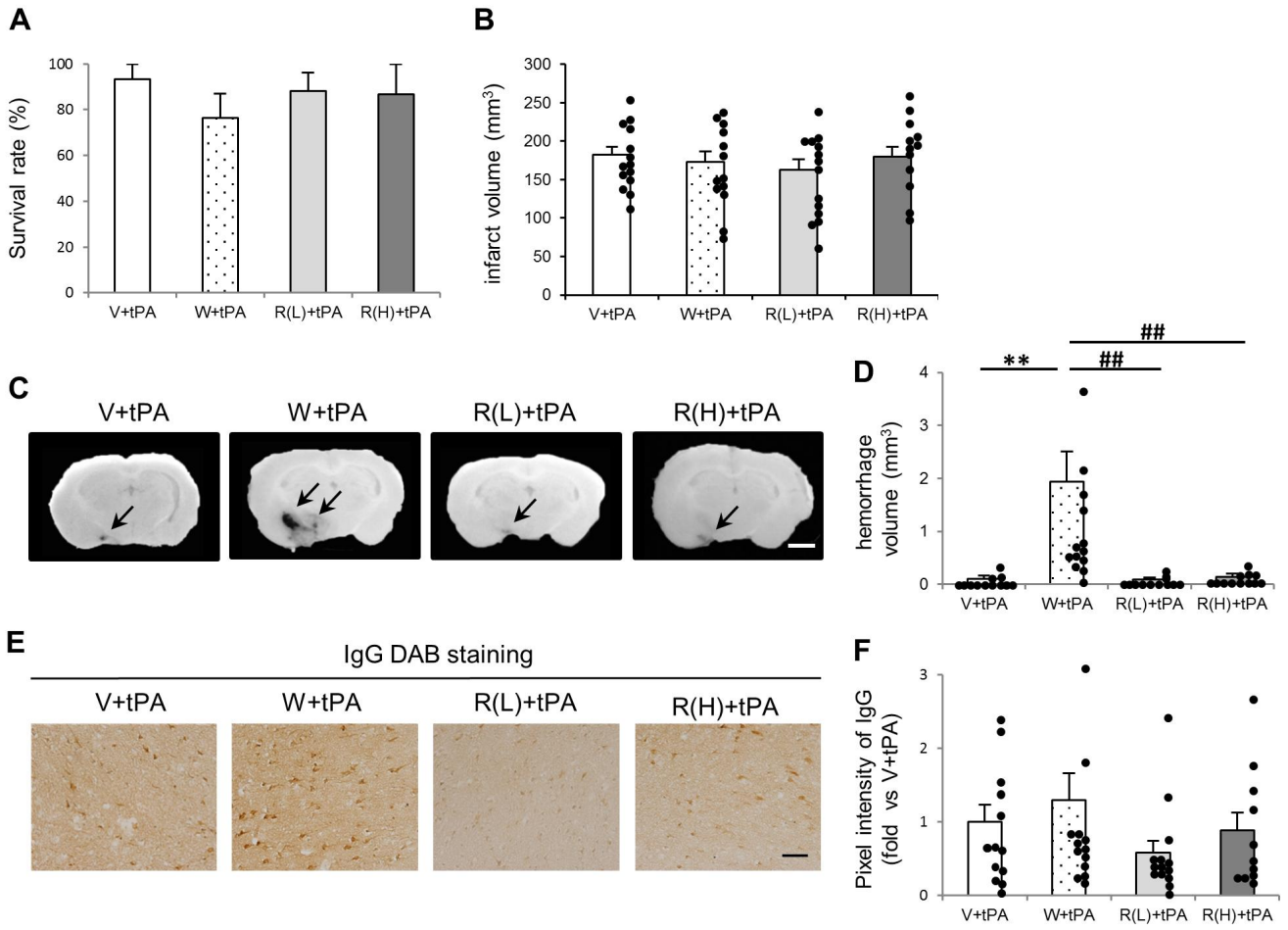


Fig 4.

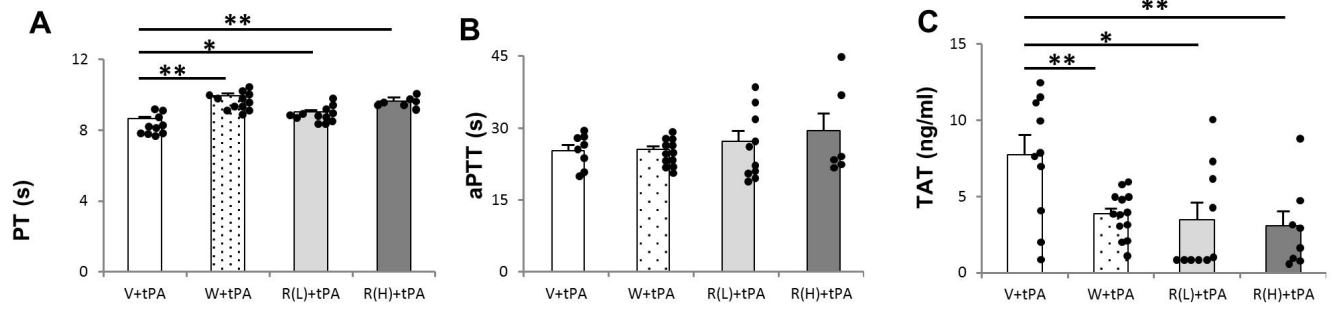


Fig. 5

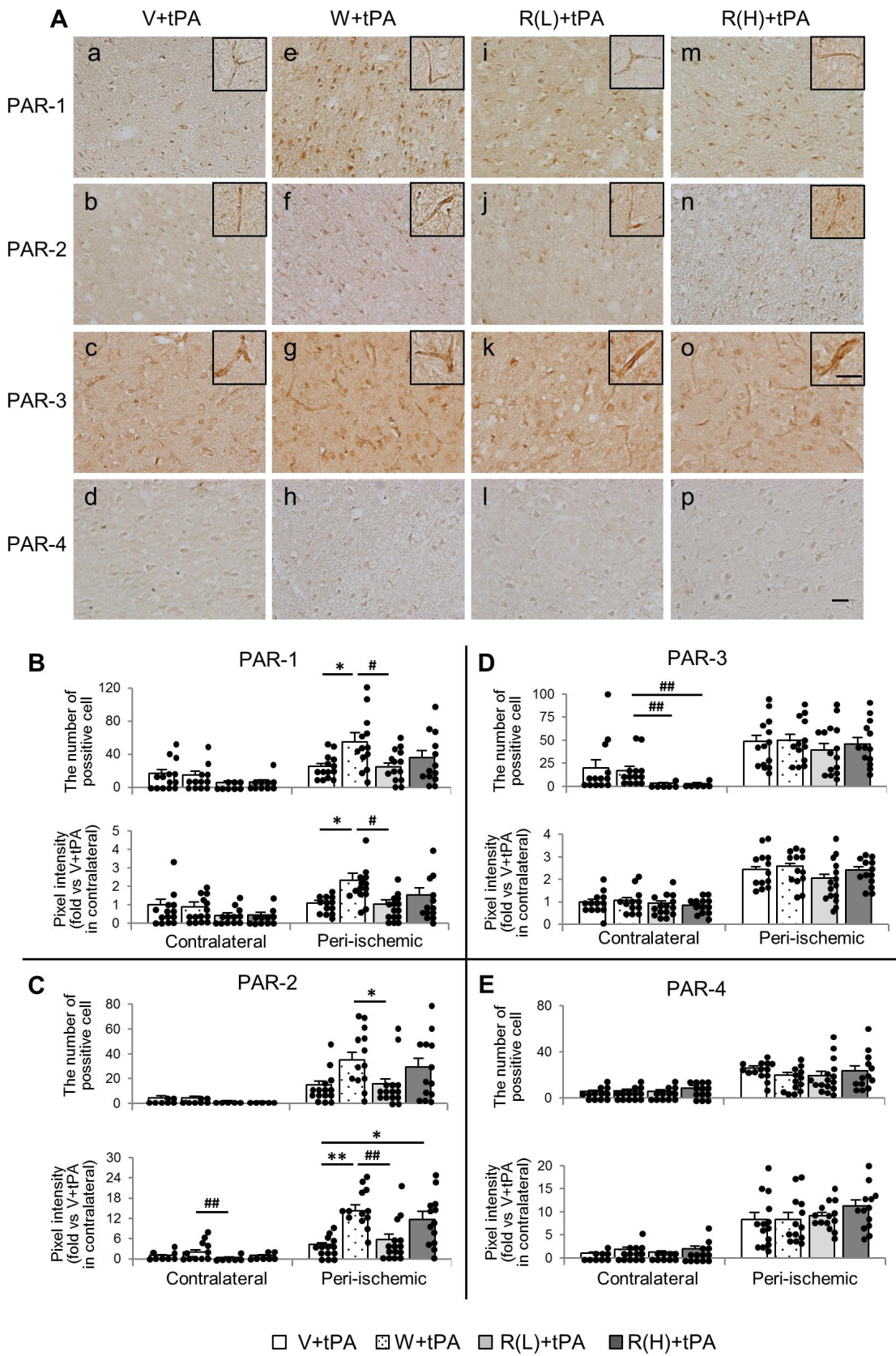


Table I. Primary Antibodies Used

| Antibody | Description of immunogen | Source, host species, catalog No., RRID | Concentration used |
|------------|------------------------------------------------------------------------------------------|------------------------------------------------------------------|--------------------|
| rat-IgG | antibodies recognizes both rat-IgG heavy and light chains | Vector Laboratories, rabbit, BA-4000, AB_2336206 | 1:500 |
| PAR-1 | epitope mapping within amino acids 42-55 of thrombin receptor of human origin | Santa Cruz Biotechnology, mouse monoclonal, sc-13503, AB_2101175 | 1:50 |
| PAR-2 | epitope mapping within amino acids 37-50 of PAR-2 of human origin | Santa Cruz Biotechnology, mouse monoclonal, sc-13504, AB_628101 | 1:50 |
| PAR-3 | epitope mapping at the C-terminus of PAR-3 of mouse origin | Santa Cruz Biotechnology, goat polyclonal, sc-8209, AB_2101327 | 1:50 |
| PAR-4 | epitope mapping at the C-terminus of PAR-4 of mouse origin | Santa Cruz Biotechnology, goat polyclonal, sc-8462, AB_2159244 | 1:50 |
| NeuN | recombinant fragment corresponding to Human NeuN aa 1-100 (N terminal). | Abcam, rabbit polyclonal, ab104225, AB_10711153 | 1:500 |
| LEL | a stable single subunit glycoprotein containing about 50 percent arabinose and galactose | Vector Laboratories, B-1175, AB_2315475 | 1:200 |
| GST- π | purified human glutathione S-transferase pi | MBL, rabbit polyclonal, 312, AB_591792 | 1:500 |
| GFAP | GFAP isolated from cow spinal cord. | Dako, rabbit polyclonal, Z0334, AB_10013382 | 1:1000 |
| Iba-1 | synthetic peptide corresponding to C-terminus of Iba1 | Wako, rabbit polyclonal, 019-19741, AB_839504 | 1:1000 |